Polymer Bulletin (2024) 81:1803–1820
https://doi.org/10.1007/s00289-023-04787-5

ORIGINAL PAPER

Investigation on the influence of PEG end groups on the ring-banded spherulite morphology of PEG/PLLA blends

Wei-Chi Lai[1] · Wen-Bin Liau[2] · Ling-Yueh Yang[2,3] · Tai-Tso Lin[2]

Received: 16 September 2022 / Revised: 22 March 2023 / Accepted: 30 March 2023 /
Published online: 15 April 2023

Abstract

The morphology and microstructure of crystalline blends of poly (ethylene glycol) (PEG) and poly (L-lactic acid) (PLLA) were examined using polarized optical microscopy (POM) and scanning electron microscopy (SEM). As PEG was in the melt state during PLLA crystallization, it was rejected from the PLLA bundles. The size of PEG inclusions determined by their extraction is around 1 μm. The PEG/PLLA blends exhibited not only spherulites with Maltese crosses but also distinct extinction rings. The formation of ring-banded spherulites and the periodic distance between the rings were related to the degree of supercooling of the polymer. The ring-banded structure was easily obtained at a high PEG content (70 wt%) and high PLLA crystallization temperature (120 °C). The end group of PEG significantly affected the morphology of PEG/PLLA blends. PLLA blended with PEG containing both end groups as CH_3 exhibited the greatest melting temperature depression and lowest degree of supercooling of PLLA, implying the formation of ring-banded spherulites with the smallest PEG content (30 wt%) and lowest PLLA crystallization temperature (85 °C). PEG morphology was also observed using POM after the formation of PLLA crystals. Because PLLA crystals confined the formation of PEG crystals, the chain growth direction of PEG was in association with that of PLLA. Therefore, a brighter POM image was obtained on PEG crystallization.

Keywords PEG · PLLA · Blend · Morphology · End group

✉ Wei-Chi Lai
wclai@mail.tku.edu.tw

[1] Department of Chemical and Materials Engineering, Tamkang University, No.151, Yingzhuan Rd., Tamsui Dist., New Taipei 25137, Taiwan R.O.C.

[2] Department of Materials Science and Engineering, National Taiwan University, No.1, Roosevelt Rd. Sec. 4, Taipei 10617, Taiwan R.O.C.

[3] Present Address: Composite Materials Section, Materials and Electro-Optics Research Division, National Chung-Shan Institue of Science and Technology, Lung-Tan, P.O. Box 90008-8-2, Tao-Yuan 32599, Taiwan R.O.C.

Introduction

In the recent decades, polymer blends have been well studied and documented by industrial and scientific research [1–3]. The applications of polymer blends in commercial utilities have gradually attracted increasing attention. Among them, some recently proposed applications for polymer blends include immobilizing enzyme biocatalysts, drug delivery systems, gas separation membranes, and cardiovascular implants [4–7].

To date, a variety of miscible polymer blends have been examined. Most research dealing with polymer blends have emphasized binary systems consisting of amorphous/amorphous and amorphous/crystalline components [8, 9]. However, mixtures containing two crystalline compositions are seldom studied. Investigation on two crystalline polymers wherein both components can crystallize is more complicated. Crystallization involving two different crystalline polymers, each within its specific temperature regime and time period, is of particular interest in the applications such as gas separation membranes and food packaging [10, 11]; for example, the gas permeability behaviors can be tuned by the efficient control of crystallization conditions of the blends. Therefore, such binary crystalline systems can provide various crystalline conditions for intensive research on the morphologies and crystallization behaviors of miscible polymer blends.

Until now, several polymer blends containing two crystalline components have been investigated and documented; for instance, one of the most studied materials is polyethylene/polypropylene blend, which has attracted considerable industrial attention due to its wide application in packaging [12]. Poly (L-lactic acid) (PLLA) is a well-known biodegradable crystalline polymer and has been widely used for commercial applications due to its renewability, high biocompatibility, and low toxicity for the human body and environment [13]. The drawbacks of PLLA include low crystallization rate, brittleness, and hydrophobicity, thereby restricting its wider applications [14]. Several preparation approaches like grafting, copolymerization, and blending were proposed to improve these physical properties of PLLA [15–17]; among these, the most economic and efficient method is polymer blending.

Poly(ethylene glycol) (PEG) exhibits hydrophilicity and is a flexible biocompatible crystalline polymer. Blends of PLLA with PEG have been previously extensively developed and investigated to improve the mechanical properties and biodegradation of PLLA [18–21]. In addition, the small amount of PEG can act as a plasticizer to increase the PLLA crystallization rate [22]. Through many studies, it has been reported that PEG/PLLA blends are miscible in the melt, and the crystallization behavior of PLLA is significantly influenced by the addition of PEG [23–25]. PEG/PLLA blends have been developed for commercial use with the majority market being food packaging applications [26]. Furthermore, owing to their compatibility and biodegradability, and the extensive research in biomedical fields in recent years, an increase in the applications of PEG/PLLA blends in drug delivery systems and tissue engineering scaffolds is expected [27].

As mentioned earlier, many studies have investigated the miscibility and physical properties of PEG/PLLA blends. However, to the best of our knowledge, only

one study (conducted by us) investigated the blends of PLLA with different end groups of PEG [23]. The chemical structures of these end groups of PEG are shown in Fig. 1. The results demonstrated that the effect of the end groups of PEG significantly affected the miscibility and crystallization behaviors of PEG/PLLA blends. Herein, we provide further physical insights into the influence of PEG end groups on the microstructures and morphologies of the PEG/PLLA blends. In view of the concept that material properties are determined by their structures, it is believed that an understanding of structures is important and deserves investigation in the present study.

Usually, the morphology of polymer blends depends on the crystallization rate and diffusion rate of the non-crystallizable component. The crystallization kinetics in such crystalline/crystalline blends depend on the morphology resulting from prior crystallization of the other component. Thus, it is expected that the crystallization kinetics and morphology in binary crystalline systems could reveal new insights. This study mainly focused on the spherulitic morphology and microstructure observed for a series of PEG/PLLA blends as evidenced by polarized light optical microscopy (POM) and scanning electron microscopy (SEM). In addition, the effect of different end groups of PEG on the morphology and microstructure of PEG/PLLA blends is also discussed. Furthermore, it is known that the periodicity in ring-banded spherulites usually depends on the chain mobility or the degree of supercooling. The results of this study indicate that the formation of ring-banded structures strongly depend on the degree of supercooling of the blends. The dependence of the banding phenomenon has been investigated in many crystalline polymers. This study may be the first to discuss these observations in PEG/PLLA blend systems.

For the potential application, the ring-banded structures have been developed as "templates" to fabricate ordered and interpenetrated nanoporous polymeric materials [28, 29]. The noncrystalline components are simultaneously excluded out by the twisted crystalline lamellae during the crystallization process. The highly ordered and periodic rings which consisted of 3-D interconnected nanopores can be obtained by removing the noncrystalline components. Most researchers have used block copolymers and anodic aluminum oxide (AAO) as templates to prepare ordered

Sample	Chemical Structure
PEG(2OH)	$H+O-CH_2-CH_2+_nO-H$
PEG(1OH-1CH3)	$H+O-CH_2-CH_2+_nO-CH_3$
PEG(2CH3)	$CH_3+O-CH_2-CH_2+_nO-CH_3$

Fig. 1 Chemical structures of PEG used in this study

porous polymeric materials [30, 31]. In this study, we investigated the banded spherulites appeared in the PEG/PLLA blends. PEG is cheap, eco-friendly and easily removal by water. Therefore, ordered porous PLLA may be further obtained, having potential applications in cartilage regeneration, drug delivery, and tissue engineering [32, 33].

Materials and methods

Materials

PEG(2OH), PEG(1OH-1CH_3), and PEG(2CH_3) were obtained from Aldrich Co. (USA) and had a weight-average molecular weight of 2000 g/mole. The PLLA sample was purchased from Polysciences Co. (USA), and its weight-average molecular weight was 200 000 g/mole. The glass transition temperature (T_g) and melting temperature (T_m) of PEG are around − 62 and 58 °C, respectively. The corresponding temperatures of PLLA were 62 °C and 180 °C.

Preparation of blends

All samples used in this study were prepared by solution-casting method. Specific amounts of PEG and PLLA were dissolved in chloroform yielding a 2% (0.4 g polymer blends/20 ml solvent) solution according to the desired composition. The blend ratios were calculated by weight. For the observation of banded spherulites, the PEG/PLLA 30/70, 50/50 and 70/30 were chosen. Then, the solution was cast into a glass Petri dish (diameter 50 mm). A cast film (approximately 200 μm thick with a diameter of 50 mm) was obtained after gradually evaporating most of the chloroform solvent at room temperature. The film was further dried in vacuum at 80 °C for 24 h. Note that if a Petri dish was used with a diameter larger than 50 mm, it would be difficult for PEG/PLLA 70/30 to form a film due to the sample brittleness. In addition, our previous study has verified no measurable residual solvent in these blends [23].

Characterization

The spherulitic morphologies of PEG/PLLA blends were monitored using a polarizing optical microscope (POM, HFX-DX, Nikon, Japan). The samples were placed on cover glasses, heated to 180 °C and held for 3 min on a hot stage (THMS600, Linkam, UK). The samples were then quickly cooled to their crystallization temperature, where the resultant morphology was observed.

The surface microstructures of PEG/PLLA blends were observed using JEOL JSM-6300 scanning electron microscopy (SEM, JSM-6300, JEOL, Japan). PEG and PLLA with an intended composition were dissolved in chloroform. The following solution was then taken out and dropped on the glass slide. The thin film was obtained after solvent evaporation. The sample (thin film) was first melted on the

aforementioned hot stage at 180 °C for 3 min. The sample was then quickly cooled to their crystallization temperature.

Results and discussion

Phase behavior

To facilitate the understanding of the morphology and microstructure of PEG(2OH, 1OH-1CH_3, and 2CH_3)/PLLA blends investigated in this study, some previous results [23] on the thermal behavior of blends over the entire composition range are listed in Fig. 2. From our previous study [23], the PEG/PLLA blend system shows a composition-dependent single T_g with the weight ratio of 10/90. Blending PEG with PLLA increases the PLLA crystallization rate. Thus, the recrystallization peak of PLLA does not appear after the quenching process except for the 10/90 composition. The melting temperatures (T^o_m) reported in Fig. 2 refer to the equilibrium melting temperatures obtained from Hoffman–Weeks analysis. The equilibrium melting temperature of the crystalline component in a blend is lower than that of the neat crystalline polymer due to the thermodynamically favorable interactions when the blend is miscible [34]. The equilibrium melting temperature of PLLA decreases as component PEG increases, indicating that PEG/PLLA blends are thermodynamically miscible in all compositions. The effect of different end groups of PEG on PEG/PLLA

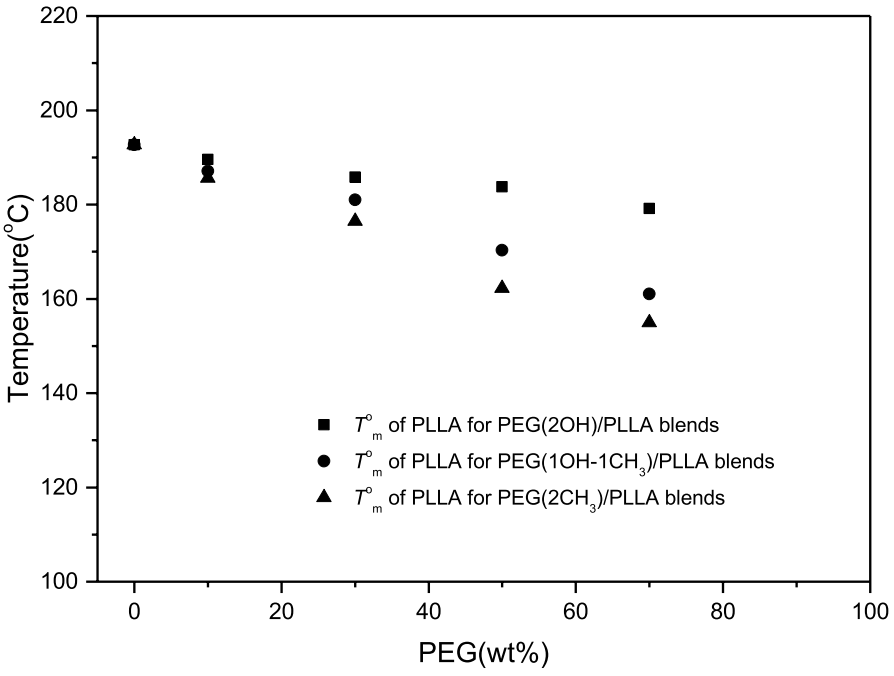

Fig. 2 Thermodynamic behavior of PEG/PLLA blends [25]

blends is also discussed. PLLA blended with PEG containing two OH end groups exhibits the smallest melting temperature depression, indicating worst miscibility. It is expected that the OH groups of PEG easily form intra-molecular hydrogen bonding, whereas the interactions with PLLA are not sufficiently strong, thereby resulting in a weak miscibility of PEG and PLLA.

Morphology and microstructure

Both PEG and PLLA are crystalline polymers; in this system, they involve two crystallization conditions. One involves the observation of PLLA morphology and microstructure before PEG crystal formation, and the other involves the observation of PEG morphology and microstructure after PLLA crystal formation. For the measurement of morphology and microstructure of PEG/PLLA blends, POM and SEM instruments were used to examine.

First, the PLLA morphology and microstructure are observed before PEG crystal formation. Figure 3a–e shows the spherulitic morphologies of different compositions of PEG(1OH-1CH_3)/PLLA blends isothermally crystallized at 120 °C using POM, where only PLLA crystallizes from the blends under the experimental condition. PEG acts as a non-crystallizable component in these blends. Similar results were found in blends with different PEG end groups and were thus not shown. The PLLA morphology (Fig. 3a) is that of conventional Maltese crosses with a birefringent pattern. The irregularity of the texture of the PLLA spherulites increases with the amount of PEG, which might follow from the coarseness of the crystalline lamellae. The coarseness of the texture is suggested to be due to melt PEG trapped in PLLA spherulites. Therefore, the blend could exhibit interlamellar or interfibrillar morphology. Additionally, the spherulites completely fill the space at the final crystallization stage. Our previous study has demonstrated the variation of PLLA spherulite radius with time was linear, implying that the crystallization environment at the growth front was the same during the PLLA crystallization [23]. Besides, SEM is also used to examine the surface microstructure of PEG/PLLA blends. Figure 4 presents the SEM micrograph of PEG(1OH-1CH_3)/PLLA 30/70 blend, which was first heated to 180 °C, held for 3 min, and then cooled to 100 °C to ensure complete formation of PLLA crystals. Figure 4 indicates a bright feature at the surface of the blend. However, whether it indicates PEG or PLLA could not be ascertained. Therefore, in this study, ethanol was used as a solvent to extract PEG from the PEG/PLLA blend. Figure 5 shows the SEM micrograph of extracted PEG from PEG/PLLA 30/70 and 70/30 blend, and it confirms that PEG samples are found at the surface. For the PEG/PLLA 70/30 system, the width of the hole (one is indicated by the arrow in Fig. 5b) after PEG is extracted is ~ 1 μm, implying that PEG is not trapped in the PLLA interlamellar regions. The distance of the segregation in lamellar regions should be close to hundreds of Å. Therefore, PEG is rejected from the PLLA bundles, and the blend exhibits interfibrillar segregation (see the schematic representation in Fig. 6).

Figure 3b–e shows that after blending with PEG, the spherulites of PLLA exhibit different morphology than that by pure PLLA. Ring-banded spherulites were

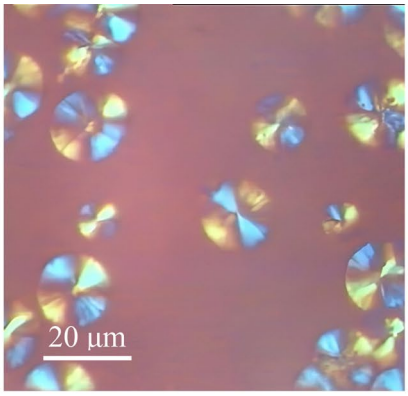

(a) PLLA

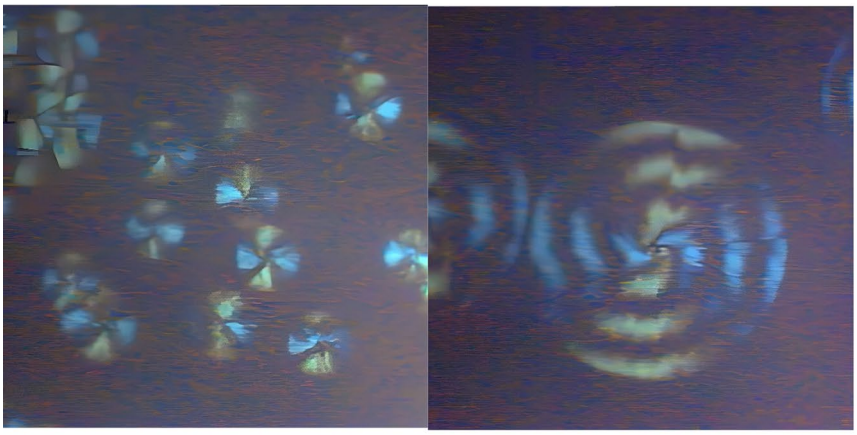

(b) 10/90 (c) 30/70

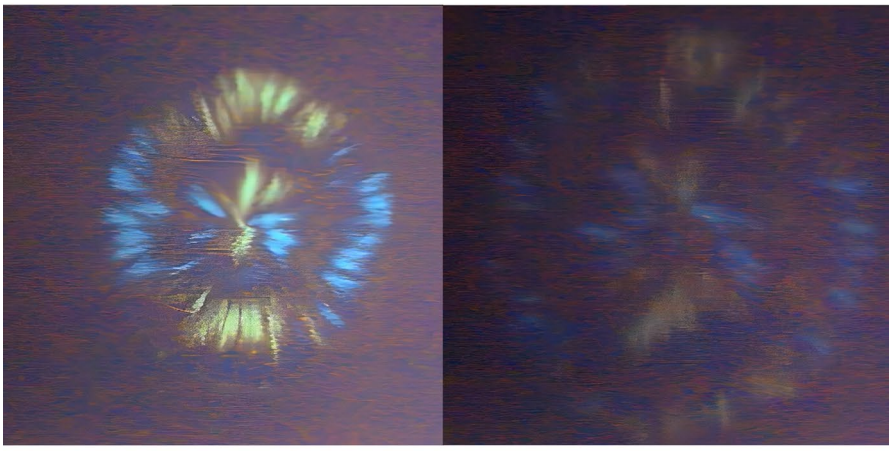

(d) 50/50 (e) 70/30

Fig. 3 **a–e** POM micrographs of different compositions of PEG(1OH-1CH_3)/PLLA blends isothermally crystallized at 120 °C

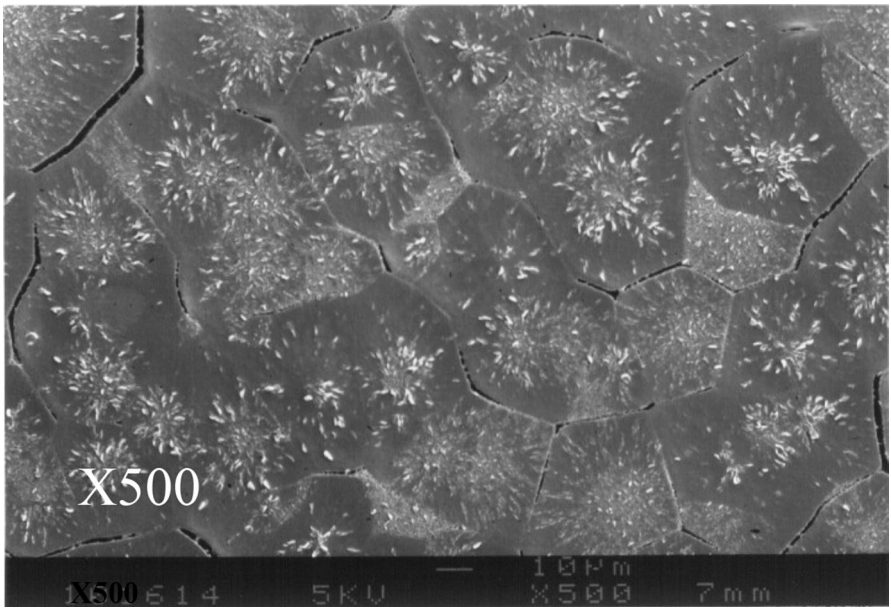

Fig. 4 SEM micrographs of PEG(1OH-1CH_3)/PLLA 30/70 blend isothermally crystallized at 100 °C

observed for the blends. The appearance of banded spherulitic structures have also been observed in the blends of poly (ethylene adipate) (PEA)/poly (butylene succinate) (PBS), poly (aryl ether ketone) (PAEK)/poly (aryl ether ether ketone) (PEEK), and poly (ε-Caprolactone) (PCL)/ poly (vinyl butyral) (PVB), whereas such structures did not appear for the pure crystalline polymer component [35–37]. The formation mechanism of banded spherulites has attracted intensive study in the past decades, but controversy still remains [38, 39]. The most accepted explanation of these morphological structures is lamellar twisting model [40, 41], where the crystalline lamellae periodically twist along the radial growth direction of the spherulites. The change of birefringence, associated with the change of crystalline lamellar orientation, leads to the banded features observed using POM. The main driving force of lamellar twisting is attributed to the unbalanced anisotropic surface stresses [42, 43], of which the distribution is affected by the molecular chirality and chemical groups on lamellar surface. As seen in Fig. 3, the formation of such a pattern in PEG/PLLA blends implies the presence of PEG that has altered the aggregation and twisting of the PLLA lamellae. It should be noted that pure PLLA has been found to exhibit ring-banded spherulites at certain molecular weights and crystallization temperatures [44, 45].

The spherulitic morphologies of PEG(1OH-1CH_3)/PLLA 50/50 blend films at different crystalline temperatures (T_c) by POM are shown in Fig. 7a–d. In this study, the formation of PLLA spherulites was not suppressed when the crystallization temperature was less than 85 °C; on the other hand, the spherulitic growth rate was very slow at crystallization temperature above 130 °C. Thus, the POM experiments were performed between 85 and 130 °C. The conventional PLLA

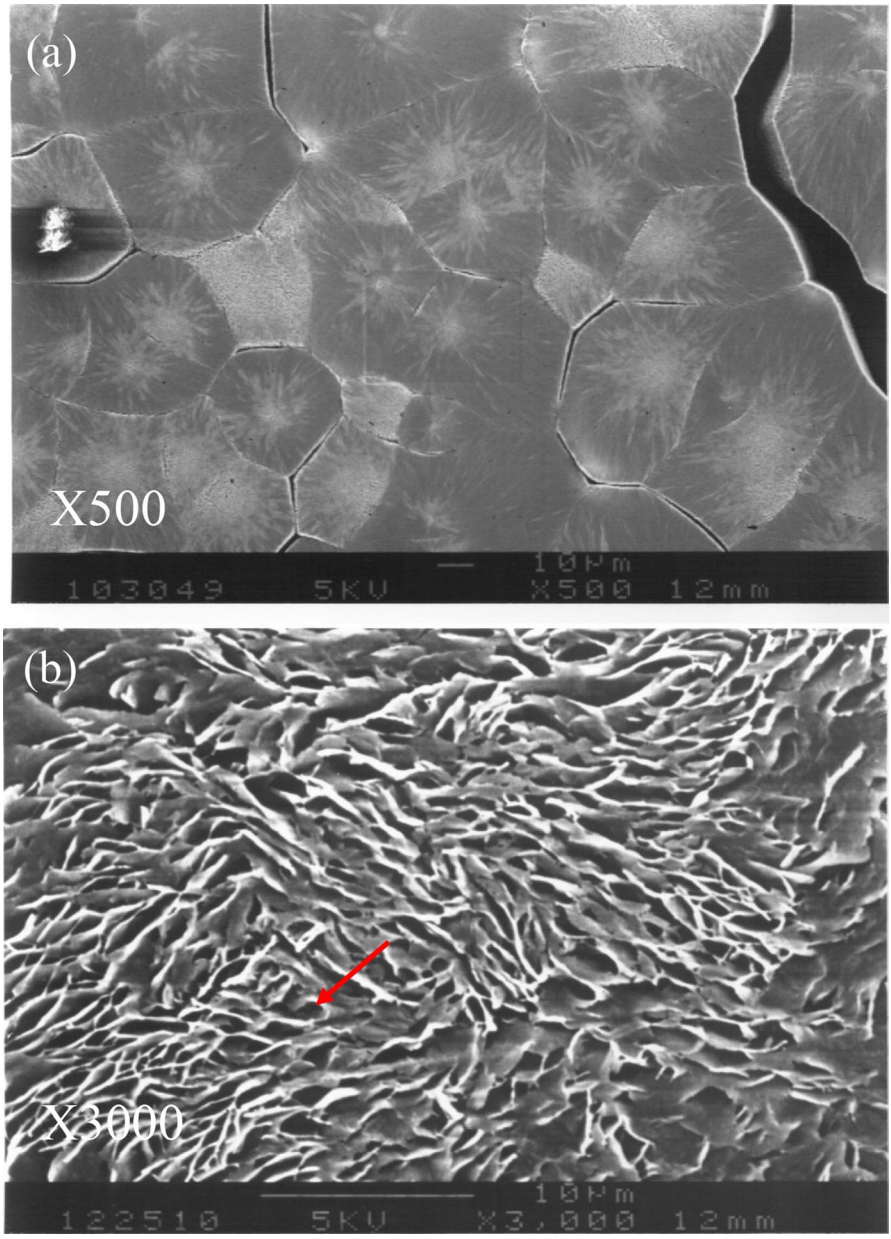

Fig. 5 SEM micrographs of extracted PEG from PEG/PLLA **a** 30/70 and **b** 70/30 blend isothermally crystallized at 100 °C

spherulite transforms into the ringed-banded spherulite at T_c from 90 to 100 °C. Figure 1 shows that the equilibrium melting temperature of PLLA decreases as PEG content increases, reducing the degree of supercooling ($\Delta T = T^{o}_{m} - T_c$) of

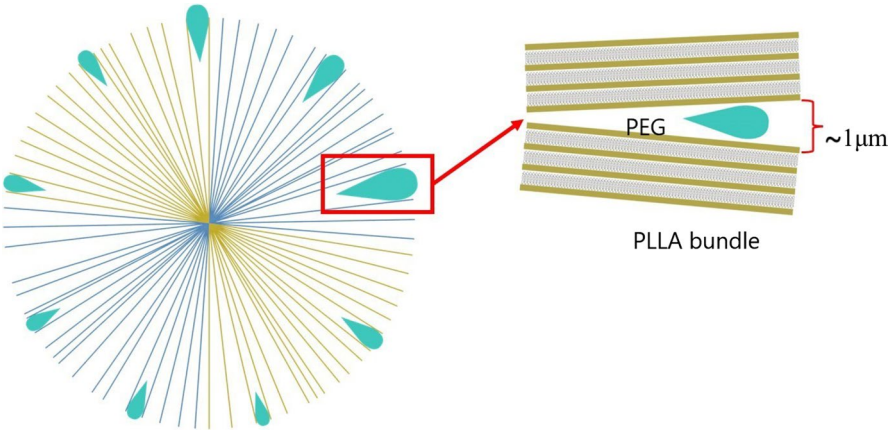

Fig. 6 Schematic representation of the interfibrillar segregation in PEG/PLLA blend

PLLA. Additionally, the increment of the T_c of PLLA implies that the T_c is closer to the T^o_m of PLLA, and indicates the reduction in the degree of PLLA supercooling. Hence, it is inferred that the morphology of spherulites is related to the degree of supercooling of the polymer. A lower degree of polymer supercooling corresponds to an easier formation of ring-banded structure. At low crystallization temperature and large degree of supercooling, the increased spherulitic growth rate resulted in the insufficient time to accomplish the cooperative lamellar twisting [46]. In addition, the high nucleation density was also not favorable for the formation of the ring structures [44].

In addition, a periodic distance of the ring-banded spherulites is observed. The periodic distance of the ring-banded spherulites of the blend (ρ) is defined as the distance between the centers of two bright bands. The periodic distance of extinction rings was all measured after the complete formation of PLLA spherulites, and the selected spherulites have at least one ring. Figure 8a displays the composition dependence of the periodic distance of extinction rings, which increases with increasing PEG composition for PEG(1OH-1CH_3)/PLLA blends. This result is consistent with the observation of the spherulites in poly (ε-caprolactone) (PCL)/poly (vinyl chloride) (PVC), PCL/poly (propylene fumarate) (PPF), and PCL/poly (styrene-co-acrylonitrile) (SAN) [47–49]. Figure 8b shows the periodic distance of extinction rings as a function of crystallization temperature for different PEG(1OH-1CH_3)/PLLA compositions. The periodic distance increases with the crystallization temperature, which is consistent with the results obtained by Wang et al. [47]. Figure 9 shows the periodic distance of extinction rings as a function of the parameters $T_c - T_g$ and $T^o_m - T_c$ for PEG(1OH-1CH_3)/PLLA blends. $T_c - T_g$ represents the overall mobility of the blend, and $T^o_m - T_c$ represents the degree of supercooling of the blend. The periodic distances of the ring-banded spherulites of the blend with different blend ratios lie on the master curve shown in Fig. 9b, implying that the periodic distances of the ring-banded spherulites are inherently related to the degree of

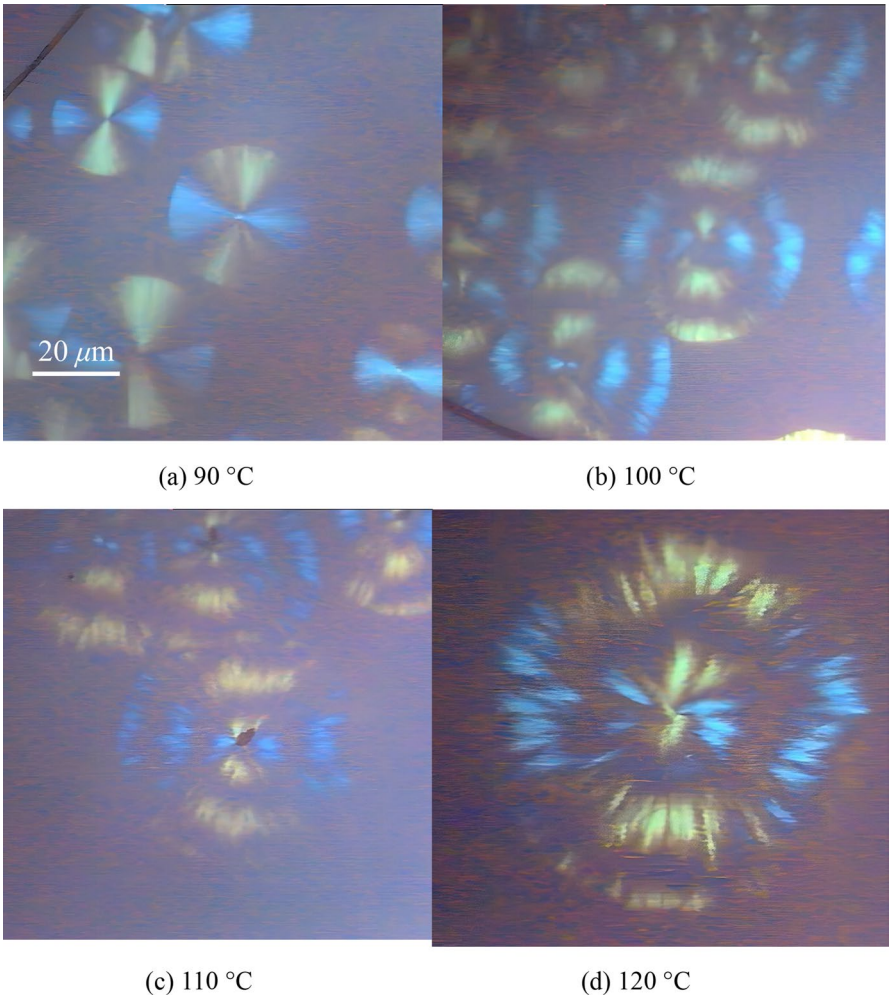

Fig. 7 **a–d** POM micrographs of PEG(1OH-1CH_3)/PLLA 50/50 blends at different crystallization temperature

supercooling of the blend. However, these results differ from those obtained by Wang et al. [47] perhaps because the compositions of the blends (PCL/SAN) used in their study differ from those of the blends used herein.

With reference to the effect end groups of PEG on the morphologies of PEG/PLLA blends, Fig. 10 shows the distribution of the spherulitic morphologies of PEG(2OH, 1OH-1CH_3 and 2CH_3)/PLLA blends. Table 1 summarizes these results. The PEG(2CH_3)/PLLA blend system has the lowest equilibrium melting temperature of PLLA (Fig. 2), and therefore also exhibits the least degree of supercooling of PLLA, indicating an easier formation of ring-banded spherulites. Thus, the PEG(2CH_3)/PLLA blend system exhibits a ring-banded structure

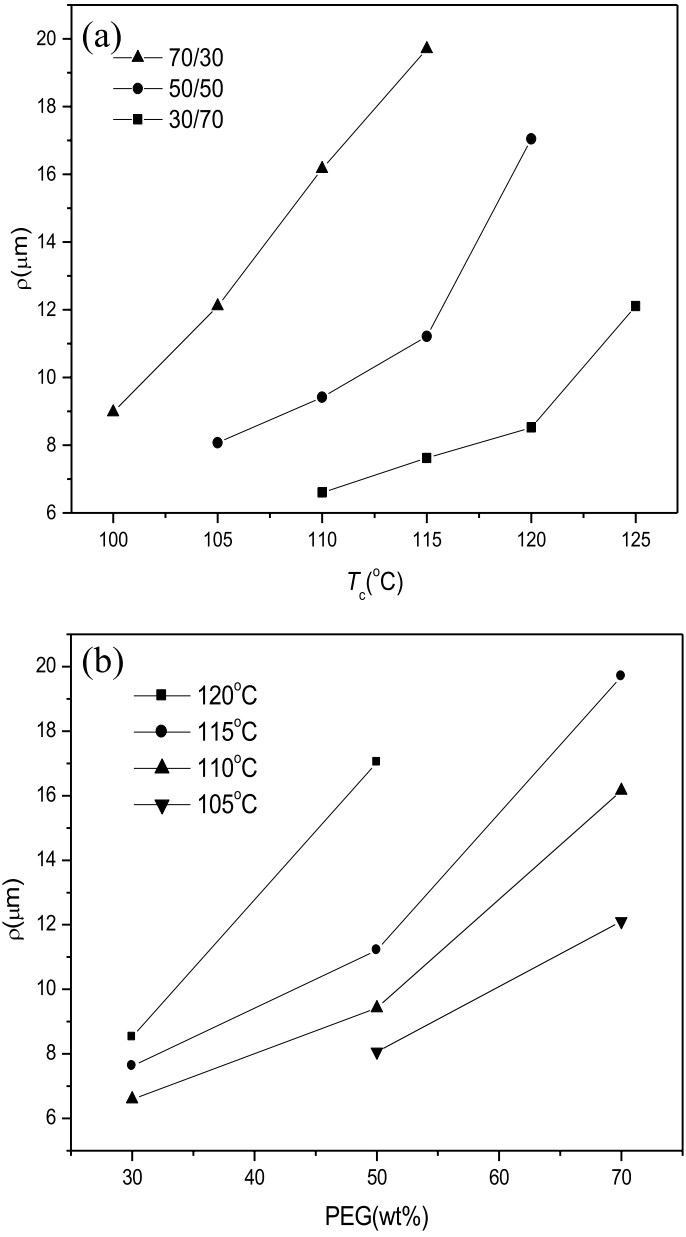

Fig. 8 Variation of periodic distance of extinction rings with **a** crystallization temperature and **b** blend composition for PEG(1OH-1CH_3)/PLLA blends

with the smallest PEG content and lowest PLLA crystallization temperature. This result reconfirms that the ring-banded structure is related to the degree of supercooling of the polymer.

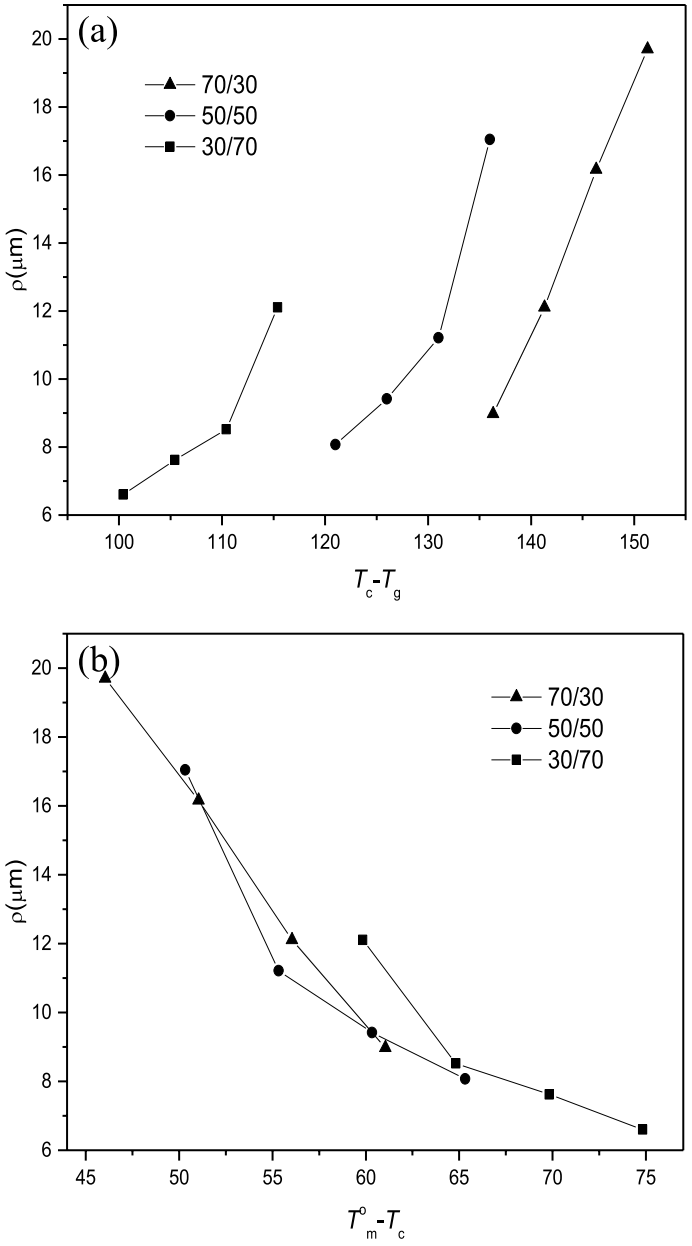

Fig. 9 The periodic distance of extinction rings as a function of **a** $T_c - T_g$ and **b** $T^o_m - T_c$ for PEG(1OH-1CH_3)/PLLA blends with different blend ratios

Second, the morphology and microstructure of PEG are observed after PLLA crystals are formed. Consider PEG(1OH-1CH_3)/PLLA, for example. Samples were first heated to 180 °C, held for 3 min, and then cooled to 120 °C until a

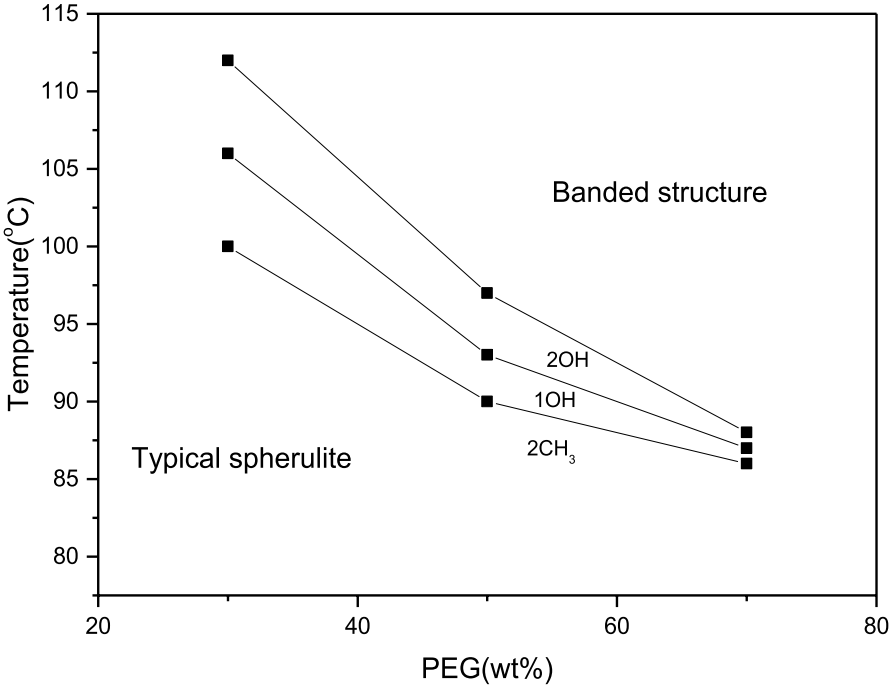

Fig. 10 Distribution of spherulitic morphologies of PEG/PLLA blends

Table 1 The transition temperature from typical spherulite to banded structure

PEG(wt%)	2OH	1OH-1CH_3	2CH_3	unit: °C
10	–	–	–	
30	112	106	100	
50	97	93	90	
70	88	87	85	

–: No banded structure

complete formation of PLLA crystals was achieved. Then, the samples were quickly quenched to 25 °C and the morphology of PEG was observed. Figure 11 shows the blend morphologies after such conditions were applied, using POM for 2 s per image. The images obtained by POM indicate bright features. However, the typical spherulites of PEG are not observed. Moreover, the shape of the hole after PEG extraction by ethanol is not round (Fig. 5). Therefore, the bright features do not indicate PEG spherulites. Spherulites are typically observed as Maltese crosses; nevertheless, some parts of the image are brighter than the others, perhaps because the PLLA crystal constrains the formation of PEG crystal. The brightened image under crossed polars was also found in PEG/PLLA copolymer and blend systems by Shin et al. [48] and Banpean et al. [49]. Shin et al.

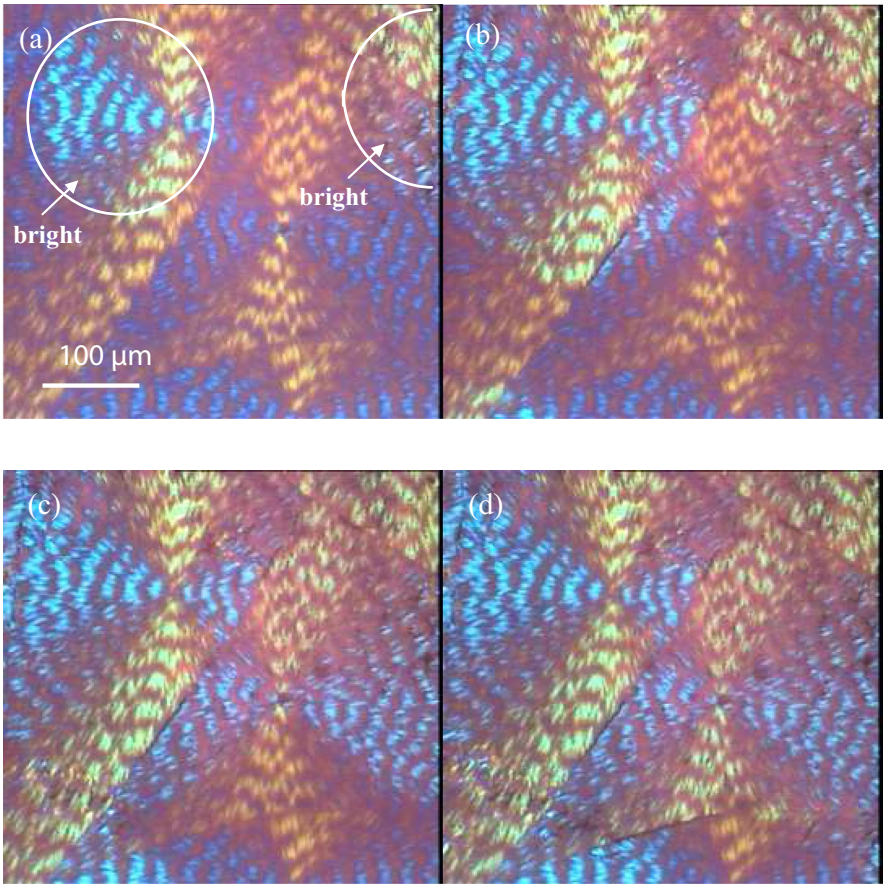

Fig. 11 POM micrographs of PEG(1OH-1CH_3) /PLLA 50/50 blend at $T_c = 25$ °C after crystallization of PLLA at 120 °C (from **a**–**d** for 2 s per image)

[48] found that the retardation of polarized light was additive, and the sign of the spherulite was conserved as poly (ethylene oxide) (PEO) crystallized within the framework of the PLLA crystals for the PLLA-b-PEO-b-PLLA triblock copolymer systems. The PEO lamellae were confined between the PLLA lamellae. Recently, confined crystallization of PEG in the pre-formed PLLA spherulite was also investigated in blend systems by Banpean et al. [49]. The PEG lamellae were oriented parallel to the preformed lamellae of PLLA. In addition, we believe PEG lamellae existed in the dark regions as well, though the brightness of the regions was not enhanced because of the orientation. In this study, PEG crystallization is strongly templated by the existing PLLA crystalline lamellae. The chain growth direction of PEG is in association with that of PLLA. Therefore, the birefringence of PLLA does not interfere with that of PEG. Hence, it is inferred that the formed PEG crystals increases the brightness of light regions of the image obtained using POM.

Conclusions

The PEG/PLLA blend is an interesting system wherein both components could crystallize. The observations of morphology and microstructure of PLLA before PEG crystal formation using POM indicate that the PLLA spherulites contacted each other and almost filled the space at the final crystallization stage. SEM observations indicate that melt PEG could be excluded out of the PLLA bundles. The morphology of ring-banded spherulite of PLLA in PEG/PLLA 30/70, 50/50 and 70/30 blend was observed under POM. Both the formation of ring-banded spherulites and the periodic distance between rings of ring-banded spherulites are related to the degree of supercooling of the blend. The analyses of the effect of different end groups of PEG on the morphology and microstructure of PEG/PLLA blends suggest that the PEG($2CH_3$)/PLLA blend system form a ring-banded structure with the smallest PEG content and lowest PLLA crystallization temperature owing to the smallest degree of supercooling of PLLA. On the other hand, the morphology and microstructure of PEG were observed after PLLA crystal formation. As PEG crystallized, the PLLA crystals confined the formation of PEG crystals. The chain growth direction of PEG was in association with that of PLLA. Thus, it is inferred that the formed PEG crystals are the brighter regions of the image obtained using POM. In the current study, we provide further physical insights into the influence of PEG end groups on the microstructures and morphologies of the PEG/PLLA blends. Our results could be used to further tune the microstructures of the blend films and provide diversity in different applications, such as templates for nanoporous polymeric materials.

Acknowledgements We gratefully acknowledge financial support from the Ministry of Science and Technology of Taiwan.

Declarations

Conflict of interest The authors declare no conflict of interest.

References

1. Robeson L (2014) Historical perspective of advances in the science and technology of polymer blends. Polymers 6:1251–1265
2. Xie L, Zhu Y (2018) Tune the phase morphology to design conductive polymer composites: a review. Polym Compos 39:2985–2996
3. Shamsuri AA, Jamil SNAM (2021) Application of quaternary ammonium compounds as compatibilizers for polymer blends and polymer composites—a concise review. Appl Sci 11:3167
4. Dubey KA, Chaudhari CV, Bhardwaj YK, Varshney L (2017) Polymers, blends and nanocomposites for implants, scaffolds and controlled drug release applications. Adv Biomater Biomed Appl 66:1–44
5. Nyamweya NN (2021) Applications of polymer blends in drug delivery. Future J Pharm Sci 7:18
6. Liberelle B, Dil EJ, Sabri F, Favis BD, Crescenzo GD, Virgilio N (2021) Immobilizing enzyme biocatalysts onto porous polymer monoliths prepared from continuous polymer blends. ACS Appl Polym Mater 3:6359–6365
7. Yong WF, Zhang H (2021) Recent advances in polymer blend membranes for gas separation and pervaporation. Prog Mater Sci 116:100713

8. Runt JP, Martynowicz LM (1986) Multicomponent polymer materials. American Chemical Society, Washington DC
9. Lee JK, Han CD (1999) Evolution of polymer blend morphology during compounding in an internal mixer. Polymer 40:6277–6296
10. Mannan HA, Mukhtar H, Murugesan T, Nasir R, Mohshim DF, Mushtaq A (2013) Recent applications of polymer blends in gas separation. Membranes 36:1838–1846
11. Sam ST, Nuradibah MA, Ismail H, Noriman NZ, Ragunathan S (2014) Recent advances in polyolefins. Nat Polym Blends Used Packag Appl 53:631–644
12. Schultz JM (2010) The crystallization and morphology of melt-miscible polymer blends. Front Chem China 5:262–276
13. Mangaraj S, Yadav A, Bal LM, Dash SK, Mahanti NK (2019) Application of biodegradable polymers in food packaging industry: a comprehensive review. J Packag Technol Res 3:77–96
14. Nofar M, Sacligil D, Carreau PJ, Kamal MR, Heuzey M-C (2019) Poly (lactic acid) blends: processing, properties and applications. Int J Biol Macromol 125:307–360
15. Lee SY, Chin IJ, Jung JS (1999) Crystallization behavior of poly(l-lactide)-poly(ethylene glycol) multiblock copolymers. Eur Polym J 35:2147–2153
16. Luckachan GE, Pillai CKS (2011) Biodegradable polymers-a review on recent trends and emerging perspectives. J Polym Environ 19:637–676
17. Farah S, Anderson DG, Langer R (2016) Physical and mechanical properties of PLA, and their functions in widespread applications—a comprehensive review. Adv Drug Deliv Rev 107:367–392
18. Sungsanit K, Kao N, Bhattacharya SN (2012) Properties of linear poly(lactic acid)/polyethylene glycol blends. Polym Eng Sci 52:108–116
19. Mohapatra AK, Mohanty S, Nayak SK (2014) Effect of PEG on PLA/PEG blend and its nanocomposites: a study of thermo-mechanical and morphological characterization. Polym Compos 35:283–293
20. Li F-J, Zhang S-D, Liang J-Z, Wang J-Z (2015) Effect of polyethylene glycol on the crystallization and impact properties of polylactide-based blends. Polym Adv Technol 26:465–475
21. Takhulee A, Takahashi Y, Vao-soongnern V (2016) Molecular simulation and experimental studies of the miscibility of polylactic acid/polyethylene glycol blends. J Polym 24:8
22. Ozkoc G, Kemaloglu S (2009) Morphology, biodegradability, mechanical, and thermal properties of nanocomposite films based on PLA and plasticized PLA. J Appl Polym Sci 114:2481–2487
23. Lai W-C, Liau W-B, Lin T-T (2004) The effect of end groups of PEG on the crystallization behaviors of binary crystalline polymer blends PEG/PLLA. Polymer 45:3073–3080
24. Li FJ, Tan LC, Zhang SD, Zhu B (2016) Compatibility, steady and dynamic rheological behaviors of polylactide/poly(ethylene glycol) blends. J Appl Polym Sci 133:42919
25. Guo J, Liu X, Liu M, Han M, Liu Y, Ji S (2021) Effect of molecular weight of poly (ethylene glycol) on plasticization of poly (L-lactic acid). Polymer 223:123720
26. Darie-Nita RN, Vasile C, Irimia A, Lipşa R, Rapa M (2016) Evaluation of some eco-friendly plasticizers for PLA films processing. J Appl Polym Sci 133:43223
27. Saini P, Arora M, RaviKumar MNV (2016) Poly(lactic acid) blends in biomedical applications. Adv Drug Deliv Rev 107:47–59
28. Ye L, Qiu J, Wu T, Shi X, Li Y (2014) Banded spherulite templated three-dimensional interpenetrated nanoporous materials. RSC Adv 4:43351–43356
29. Ye L, Shi X, Ye C, Chen Z, Zeng M, You J, Li Y (2015) Crystallization-modulated nanoporous polymeric materials with hierarchical patterned surfaces and 3D interpenetrated internal channels. ACS Appl Mater Interfaces 7:6946–6954
30. Xiang ZY, Sarazin P, Favis BD (2009) Controlling burst and final drug release times from porous polylactide devices derived from co-continuous polymer blends. Biomacromol 10:2053–2066
31. Wei Q, Fu Y, Zhang G, Yang D, Meng G, Sun S (2019) Rational design of novel nanostructured arrays based on porous AAO templates for electrochemical energy storage and conversion. Nano Energy 55:234–259
32. Tyler B, Gullotti D, Mangraviti A, Utsuki T, Brem H (2016) Polylactic acid (PLA) controlled delivery carriers for biomedical applications. Adv Drug Deliv Rev 107:163–175
33. Lu Z, Zhang B, Gong H, Li J (2021) Fabrication of hierarchical porous poly (l-lactide) (PLLA) fibrous membrane by electrospinning. Polymer 226:123797
34. Shi Y, Jabarin SA (2001) Glass-transition and melting behavior of poly(ethylene terephthalate)/poly(ethylene 2,6-naphthalate) blends. J Appl Polym Sci 81:11–22

35. Chen J, Yang D (2005) Phase behavior and rhythmically grown ring-banded spherulites in blends of liquid crystalline poly(aryl ether ketone) and poly(aryl ether ether ketone). Macromolecules 38:3371–3379
36. Wang T, Wang H, Li H, Gan Z, Yan S (2009) Banded spherulitic structures of poly(ethylene adipate), poly(butylene succinate) and in their blends. Phys Chem Chem Phys 11:1619–1627
37. Ikehara T, Kataoka T, Inutsuka M, Jin R-H (2019) Chiral nucleating agents affecting the handedness of lamellar twist in the banded spherulites in poly(ε-caprolactone)/poly(vinyl butyral) blends. ACS Macro Lett 8:871–874
38. Xu J, Ye H, Zhang S, Guo B (2017) Organization of twisting lamellar crystals in birefringent banded polymer spherulites: a mini-review. Crystals 7:241
39. Safandowska M, Rozanski A (2021) Ring-banded spherulites in polylactide and its blends. Polym Testing 100:107230
40. Ye HM, Freudenthal JH, Tan M, Yang J, Kahr B (2019) Chiroptical differentiation of twisted chiral and achiral polymer crystals. Macromolecules 52:8514–8520
41. Lovinger AJ (2020) Twisted crystals and the origin of banding in spherulites of semicrystalline polymers. Macromolecules 53:741–745
42. Wang T, Li H, Schultz JM, Yan S (2011) Morphologies and deformation behavior of poly(vinylidene fluoride)/poly(butylene succinate) blends with variety of blend ratios and under different preparation conditions. Polym Chem 2:1688–1698
43. Wen T, Sun HJ, Lotz B, Cheng SZD (2020) Scrolled/cylindrical solution-grown single crystals in form III of isotactic poly(1-butene). Macromolecules 53:7570–7579
44. Xu J, Guo BH, Zhou JJ, Li L, Wu J, Kowalczuk M (2005) Observation of banded spherulites in pure poly(L-lactide) and its miscible blends with amorphous polymers. Polymer 46:9176–9185
45. Nurkhamidah S, Woo EM (2011) Effects of crystallinity and molecular weight on crack behavior in crystalline poly(L-lactic acid). J Appl Polym Sci 122:1976–1985
46. Zhang QL, Fan JS, Feng JC (2015) Formation of banded spherulites and the temperature dependence of the band space in olefin block copolymer. RSC Adv 5:43155–43163
47. Wang Z, Wang X, Yu D, Jiang B (1997) The formation of ring-banded spherulites of poly(ε-caprolactone) in its miscible mixtures with poly(styrene-co-acrylonitrile). Polymer 38:5897–5901
48. Shin D, Shin K, Aamer KA, Tew GN, Russell TPA (2005) Morphological study of a semicrystalline poly(l-lactic acid-b-ethylene oxide-b-l-lactic acid) triblock copolymer. Macromolecules 38:104–109
49. Banpean A, Sakurai S (2021) Confined crystallization of poly(ethylene glycol) in spherulites of Poly (L-lactic acid) in a PLLA/PEG blend. Polymer 215:123370